

TITLE

# Nanocrystal: Conducting Polymer Solar Cells via a New Synthetic Route

*AUTHOR NAMES*

*Andrew A. R. Watt\*, David Blake, Halina Rubinsztein-Dunlop & Paul Meredith.*

AUTHOR ADDRESS

Soft Condensed Matter Physics Group and Centre for Biophotonics and Laser Science, School of  
Physical Sciences, University of Queensland, Brisbane, QLD 4072 Australia.

AUTHOR EMAIL ADDRESS

watt@physics.uq.edu.au

**RECEIVED DATE (to be automatically inserted after your manuscript is accepted if required  
according to the journal that you are submitting your paper to)**

CORRESPONDING AUTHOR FOOTNOTE

E-mail: [watt@physics.uq.edu.au](mailto:watt@physics.uq.edu.au), Fax: +61 7 3365 1242, Tel: +61 7 3365 1245.

ABSTRACT

In this letter we report photovoltaic devices fabricated from PbS nanocrystals and the conducting polymer poly (2-methoxy-5-(2'-ethyl-hexyloxy)-p-phenylene vinylene (MEH-PPV). This composite material was produced via a new single-pot synthesis which solves many of the issues associated with existing methods. Our devices have white light power conversion efficiencies under AM1.5 illumination of 0.7%.

## MANUSCRIPT TEXT

The first semiconductor nanocrystal:conducting polymer photovoltaic device was reported by Greenham et al. in 1996 <sup>1</sup> Since then, several groups have effectively demonstrated such devices with power conversion efficiencies under AM1.5 light of up to 1.8% <sup>2,3,4</sup> . Efficiency improvements have been mainly attributed to altering nanocrystal morphology. In all of these reports nanocrystals were synthesized separately and subsequently mixed with a conducting polymer. This approach has two shortcomings: firstly the surfactant used to prepare the nanocrystals has to be removed, some of this is incorporated into the final nanocrystal: conducting polymer mix and inhibits efficient charge transfer. Secondly, the mixing approach requires the use of co-solvents which adversely effects nanocrystal solubility and polymer chain orientation. Recently, we have developed a new nanocrystal synthesis which eliminates these synthetic problems by using the conducting polymer to control nanocrystal growth <sup>5</sup>. This paper will present our first device results from this new synthesis

Conducting polymers such as MEH-PPV have high hole mobility and low electron mobility <sup>6</sup>. Photovoltaic devices are limited by the minority carrier mobility. Hence the intrinsic carrier mobility imbalance in MEH-PPV severely limits the performance of pure polymer based photovoltaics. To overcome this imbalance, a second material is incorporated to act as an electron acceptor and pathway for electron transport. So far, the best devices have been made by incorporating C60 derivatives <sup>7</sup> and cadmium selenide semiconductor nanocrystals <sup>3</sup> into the polymer.

We have chosen lead sulphide (PbS) as our nanocrystal material because, in the quantum regime it has tunable broad band absorption <sup>8</sup>, electrons and holes are equally confined <sup>8</sup> and exhibit long excited state lifetimes <sup>9</sup>. The electron affinity ( $\chi$ ) of bulk PbS is  $\chi=3.3\text{eV}$  which is slightly larger than C60 ( $\chi=2.6\text{eV}$ ) and lower than bulk cadmium selenide ( $\chi=4.95\text{eV}$ ). Together, these properties make PbS nanocrystals a material with great potential in polymer-based photovoltaic devices.

The nanocrystal: conducting polymer composite was prepared via a method similar to reference 5. The entire reaction took place in a nitrogen dry-box as follows: A sulphur precursor solution was made by dissolving 0.1g of sulphur flakes in 5ml of toluene. In a typical synthesis, 9ml of toluene, 0.01g of MEH-PPV, 3ml of di-methylsulfoxide DMSO and 0.1g of lead acetate were dissolved in a 20 ml vial on a stirrer-hotplate. All materials were purchased from Sigma Aldrich and used without further purification. With the solution at 160 °C, 1ml of the sulphur precursor was injected. 0.2ml aliquots were taken every three minutes and injected into 2ml of toluene at ambient temperature. The reaction took approximately 15 minutes to reach completion upon which a black/brown solution resulted. The product was cleaned to remove excess lead and sulphur ions, DMSO and low molecular weight MEH-PPV by adding anhydrous methanol to cause precipitation of the composite material. The sample was centrifuged and the supernatant removed. The precipitate was then redissolved in chlorobenzene and shaken vigorously for 1 hour. The final weight percentage of nanocrystals was then determined gravimetrically. Typically we found 50-60% nanocrystals by weight.

Transmission electron microscopy (TEM) of the composite material was carried out using a Tecnai 20 Microscope. Samples were prepared by taking the cleaned product, diluting it and placing a drop on an ultra thin carbon coated copper grid (Ted Pella) with the Formvar removed. A Perkin-Elmer  $\lambda$ 40 UV-Visible Spectrophotometer was used to obtain absorption spectra of aliquots and thin films prepared by spin casting the final product on to a microscope slide.

Photovoltaic devices were fabricated as follows. A blend of poly(3,4-ethylene dioxythiophene) with poly-(styrene sulfonate) (PEDOT/PSS) was used as the anode and was spun cast twice at 2000rpm for 40 seconds onto an oxygen plasma-treated indium-tin oxide (ITO) substrate. This was then baked in a nitrogen dry-box at 150 °C for 1 hour. The nanocrystal: polymer composite material was then spun cast onto the PEDOT/PSS surface at 1500 rpm for 60 seconds. Typical film thicknesses were 60-100 nm. The films were left to dry for 30 min before aluminum cathodes were deposited by thermal evaporation at a vacuum better than  $10^{-5}$  mbar. A 5 minute anneal was carried out at 80 °C<sup>10</sup>. The active device area was 0.04cm<sup>2</sup>.

The electrical properties of devices were measured under flowing argon in an electrically shielded box. Current-voltage characteristics were measured with a Kiethley 2400 source measurement unit. Simulated solar illumination under AM1.5 global conditions was provided by an Oriel 50W Xenon Arc Lamp with AM1.5 filters at an intensity of 5mW cm<sup>-2</sup> and single wavelength excitation at 560nm through a monochromator at an intensity of 0.01mW cm<sup>-2</sup>. Quantum efficiencies were measured using a Kiethley 6435 picoammeter, Spex monochromator, Oriel 50W Xenon Arc Lamp and NIST calibrated silicon detector. All incident light intensities were measured using a NIST calibrated silicon detector.

TEM gives information concerning the nature of the nanocrystal growth and quality. Figure 1 shows that nanocrystals are formed within the polymer and they are non-aggregated with an average size of 4nm ( $\pm 2$ nm). Figure 2 shows the crystal lattice of an individual nanocrystal and demonstrates a high degree of crystallinity. MEH-PPV has an absorption edge at around 560nm and figure 3 shows how the absorption changes as PbS nanocrystals assemble as the reaction proceeds. The inclusion of nanocrystals results in an extension of the absorption into the near IR. This absorption edge corresponds to theoretical predictions for PbS nanocrystals with size between 4 and 6 nm<sup>8</sup>.

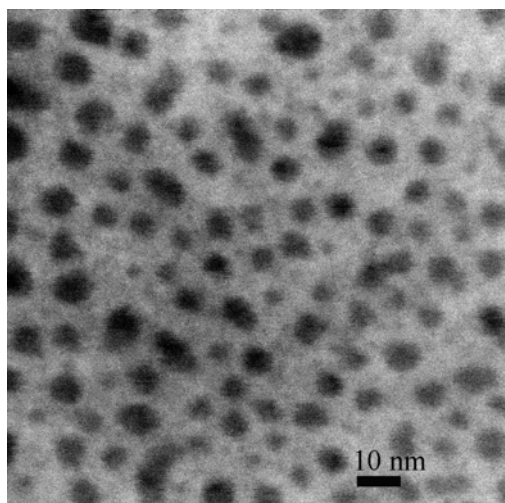


**Figure 1.** Scanning transmission electron microscopy image of a dilute sample of PbS nanocrystals.

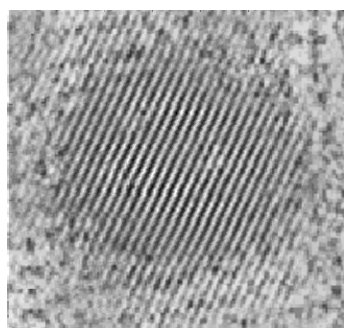


**Figure 2.** High resolution TEM image of the lattice planes in a single nanocrystal.

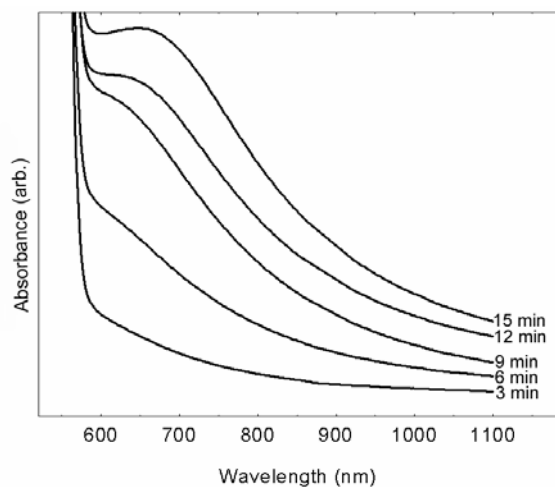


**Figure 3.** Change in absorbance as aliquots are taken as the reaction proceeds.

The current density as a function of voltage for a device in the dark and under illumination with simulated AM1.5 and at 560nm light is shown in figure 4. Device results and experimental conditions are summarised in table 1. The cell displays a relatively modest fill factor, but respectable power

conversion efficiency under white light and single wavelength illumination (0.7 and 1.1% respectively). As shown in Figure 5 the incident photon conversion efficiency (IPCE) reaches a maximum of 21% at 500nm. These results demonstrate that nanocrystals grown using the new synthesis and with equal xyz geometry can be utilized to make a device with efficiency comparable to those made from semiconductor nanocrystal rods or tetrapods. We believe that the preparation of nanocrystals in a separate surfactant and the subsequent transfer to conducting polymer is not ideal, and device optimization using our “surfactant-free” synthesis may ultimately yield higher efficiencies.

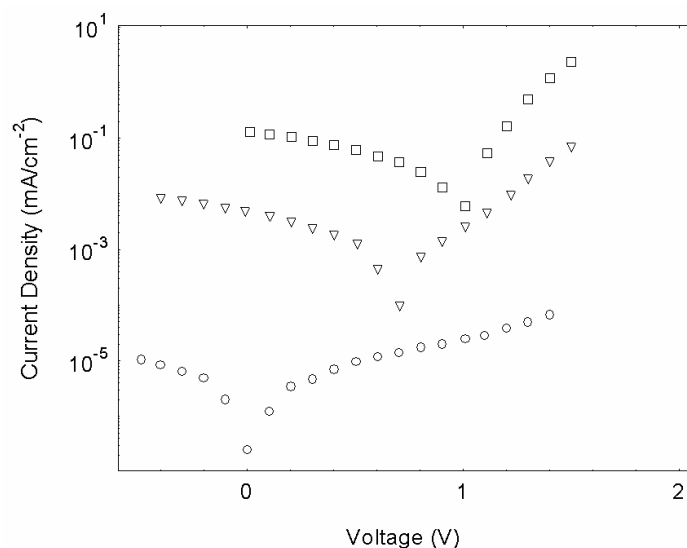


**Figure 4.** Current density vs voltage for a PbS: MEH-PPV solar cell in the dark (circles),  $0.01 \text{ mW cm}^{-1}$  illumination at 560nm (triangles) and simulated AM1.5 global light at an intensity of  $5 \text{ mW cm}^{-1}$  (squares).

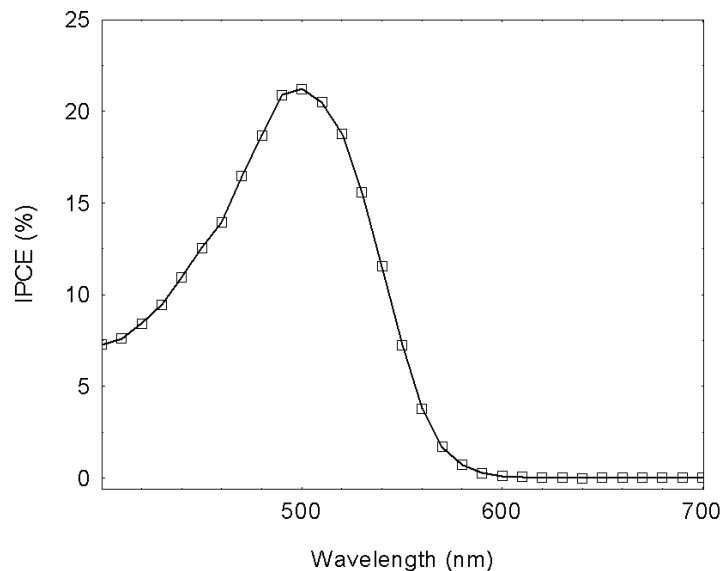


**Figure 5.** Incident photon conversion efficiency (IPCE) for a PbS: MEH-PPV solar cell.

Wavelength	560nm	AM1.5
Incident Power (mW/cm <sup>2</sup> )	0.01	5
Voc (V)	0.7	1
Isc (mA/cm <sup>2</sup> )	-0.005	-0.13
Fill Factor	0.30	0.28
Power Conversion Efficiency (%)	1.1	0.7

**Table 1.** Summary of solar cell device characteristics.

There are a number of fabrication issues to consider when making devices from our new composite: Firstly (as with most polymer-based electronic devices), the fabrication process must take place in an oxygen and water free environment, as their incorporation increases the number of charge trapping sites. Secondly, and consistent with the work presented by Padinger et al.<sup>10</sup> for the postproduction treatment of plastic solar cells, we find a 5 minute anneal just above the glass transition temperature of MEH-PPV after cathode deposition is effective in improving device performance. Thirdly, ultrasonication of the

nanocrystal: conjugate polymer product is detrimental to device performance - instead we use prolonged vigorous shaking. Finally the choice of solvent is important; films made from toluene scatter light heavily and make poor devices, whilst films cast from chlorobenzene do not. It is also important to note that the actual nanocrystal synthesis is dependent upon the solvent system used.

In conclusion we have demonstrated a plastic solar cell made from a PbS:MEH-PPV composite. Most significantly, we have shown that this new nanocrystal synthesis is effective and that nanocrystals with equal xyz geometry can be utilized to make respectable photovoltaic devices. Further efficiency improvements could be gained by tuning the nanocrystal concentration and morphology, and optimizing the active layer thickness.

**ACKNOWLEDGMENT** The work was funded by the Australian Research Council. TEM was performed at the University of Queensland Centre for Microscopy and Microanalysis.

## FIGURE CAPTIONS

**Figure 1.** Scanning transmission electron microscopy image of a dilute sample of PbS nanocrystals.

**Figure 2.** High resolution TEM image of the lattice planes in a single nanocrystal.

**Figure. 3.** Change in absorption as aliquots are taken as the reaction proceeds.

**Figure 4.** Current density vs voltage for a PbS: MEH-PPV solar cell in the dark (circles),  $0.01 \text{ mW cm}^{-1}$  illumination at 560nm (triangles) and simulated AM1.5 global light at an intensity of  $5 \text{ mW cm}^{-1}$  (squares).

**Figure 5.** Incident photon conversion efficiency (IPCE) for a PbS: MEH-PPV solar cell.

## TABLES.



Wavelength	560nm	AM1.5
Incident Power (mW/cm <sup>2</sup> )	0.01	5
Voc (V)	0.7	1
Isc (mA/cm <sup>2</sup> )	-0.005	-0.13
Fill Factor	0.30	0.28
Power Conversion Efficiency (%)	1.1	0.7

**Table 1.** Summary of solar cell device characteristics.

## REFERENCES

- (1) Greenham, N. C.; Peng, X.; Alivisatos, A. P. *Phys. Rev. B* **1996**, 54, 17628.
- (2) Liu, J.; Tanaka, T.; Sivula, K.; Alivisatos, A.P.; Frechet, J.M.J. *J. Am. Chem. Soc.* **2004**, 126, 6551.
- (3) Sun, B.; Marx, E.; Greenham N.C. *Nano Letters* **2003**, 3, 961.
- (4) Arici, A.; Sariciftci, N.S. Meissner, D. *Adv Funct Mater* **2003**, 13, 165.
- (5) Watt, A.; E. Thomsen,; Meredith, P.; Rubinsztein-Dunlop, H. accepted *Chem Commun.*  
<http://arxiv.org/abs/cond-mat/0407783>
- (6) Antoniadus, H.; Abkowitz, M.A.; Hsieh B.R. *Appl. Phys. Lett.* **1994**, 65, 2030.
- (7) Shaheen, S.E.; Brabec, C.J.; Sariciftci, N.S.; Padinger, F.; Fromherz, T.; Hummelen, J.C. *Appl. Phys. Lett.* **2001** 78, 841.
- (8) Wise, F.W. *Accounts Chem. Res.* **2000**, 33, 773.
- (9) Fernee, M.J.; Warner, J.; Watt, A.; Cooper, S.; Heckenberg, N.R., Rubinsztein-Dunlop, H. *Nanotechnology* **2004**, 15, 16.

- (10) Padinger, F.; Rittberger, R.S.; Sariciftci, N.S.; *Adv Funct Mater* **2003**, 13, 85.